

Integrating Offshore Wind Farms with Unmanned Hydrogen and Battery Ships

Sobhan Badakhshan, *Student Member, IEEE*, Soroush Senemmar, *Student Member, IEEE*,
Honglin Li, *Student Member, IEEE*, and Jie Zhang, *Senior Member, IEEE*

The University of Texas at Dallas
Richardson, TX 75080, USA

Email: {sobhan.badakhshan, soroush.senemmar, honglin.li, jiezhang}@utdallas.edu

Abstract—The transition to low-carbon electrical grids has enabled a rapid growth in offshore wind energy. In the meantime, producing green hydrogen from offshore wind farms has also gained wide attention in recent years. Among many challenges, energy transferring from offshore wind farms (especially for those in deep water) to the shoreline infrastructure has been explored in various ways. In this paper, unmanned surface hydrogen ships are explored as mobile energy resources to replace hydrogen pipelines to transfer hydrogen generated from offshore wind farms in deep water, in conjunction with unmanned battery ships for electricity transmission. The hydrogen/battery ships could charge from offshore wind farms and discharge their energy when plugged-in to the terrestrial grid or onshore hydrogen infrastructure. The schedules of the ships are optimized based on the offshore wind farm generation, weather conditions, and ship sailing timing. Results showed that by combining the hydrogen ship, battery ship, and onsite hydrogen storage tanks, more than 99% of the offshore wind farm generation could be successfully transmitted to the shore side infrastructure.

Index Terms—Unmanned Surface Vehicles, Offshore Wind Farm, Optimization, Ship to Grid, Hydrogen Ship

I. INTRODUCTION

Offshore wind energy has been growing fast in recent years due to the decreasing cost of installation, needs of energy security, and environmental concerns. The global capacity of offshore wind power has been continuously increased from 3 GW in 2010 to 23.3 GW in 2018, achieving an average increase of 29.2% annually [1]. The projected offshore wind power capacity in Europe will reach to 450 GW in 2050 [2], and the U.S. has announced a goal to deploy 30 GW of offshore wind by 2030 [3].

Electricity generated by offshore wind farms is generally transmitted to shore-side power grids using submarine cables that run from an offshore substation to onshore, grid-connected substations. The power transmission system usually connects to submarine cables with a 138-230 kV range (20–30 cm in diameter) to integrate the offshore wind farm to terrestrial networks [4]. From an environmental point of view, the installation and operation of submarine power cables may cause pollution or harmful changes to the marine environment [5]. Specifically, electric and magnetic fields of power cables in deep water that are known to be more sensitive to environmental changes, raise concerns about their environmental

impacts, since many marine organisms have magneto and electroreception abilities for vital purposes [6].

The integration of offshore wind farms and hydrogen production has been explored recently in the literature [7]. Hydrogen can fulfill the role of energy storage and even act as an energy carrier, since it has a much higher energy density than batteries and can be easily stored. Hydrogen could also be used in a variety of industry processes [8]. Hydrogen has shown the potential to be combined with offshore wind farms, which helps address challenges such as the high installation cost of electrical transmission systems [9], [10]. Offshore hydrogen pipelines have been assessed as a cost-effective way for transporting energy for large-scale and distant wind farms [11], [12]. The optimal design and economic analysis of an offshore wind-hydrogen system have been studied in [13], [14]. Green hydrogen production from offshore wind has also been investigated for ship refueling [15]. However there exist several barriers in deploying large-scale pipelines for hydrogen transport [16], such as the balance between safety and cost-effectiveness.

Alternatively, several studies have evaluated the effectiveness of hydrogen transferring by ships. For example, cargo ships were explored in [17] for transporting hydrogen tanks to participate in the optimization of offshore wind-hydrogen systems in deep water. An economic feasibility model of hydrogen production, storage, transportation, conversion, and treatment was analyzed in [18], where hydrogen ships were used for transportation. Yan et al. [19] showed that hydrogen ships could deliver the generated hydrogen with a high economic efficiency compared to the pipelines. d'Amore Domenec et al. [20] found that using ships to transport liquid hydrogen has a higher energy transport efficiency for large offshore wind farms. While most of existing work focuses on the the design and safety of hydrogen ships, less work has been explored on the optimization of the energy system operation.

An alternative way for integration of offshore wind farms is to leverage autonomous hydrogen and battery ships to transmit offshore wind electricity. The generated power from offshore wind farms could be stored in battery ships or used to produce clean hydrogen, and the automated unmanned vessels could sail to the shore and connect to the power grid or hydrogen infrastructure. The potential of deploying ships as energy vessels to transfer power of offshore wind farms

to the electrical grid, has recently received more attention [14]. For example, a robust optimization model was developed in [21] to optimize the day-ahead operations and ship-to-shore load schedules. The dynamic feasibility of connecting shipboard power systems to the grid has been assessed in [22]. A fast charging system for the battery ships was evaluated in [23], [24] for transmitting offshore wind energy to the grid. For example, Smolenski et al. [25] present an approach of ship-to-shore and shore-to-ship system synchronization, which used power converters to provide high dynamics of the synchronization and soft load transferring process, especially under distorted ship voltage conditions.

To further evaluate the feasibility and effectiveness of using unmanned vessels for the transfer of offshore wind energy, this paper co-optimizes the operations of offshore wind farms and hydrogen/battery ships. Figure 1 shows the overall framework of integrating an offshore wind farm with unmanned hydrogen/battery ships for hydrogen production and energy transportation. The problem is formulated as a mixed-integer linear programming problem, with the goal of maximizing the energy transfer from offshore farms to on-land infrastructure, by considering the vessel voyaging constraints, ports management on the shore side, operational constraints of the battery and hydrogen electrolyzer systems during the long-term operation of the hydrogen and battery ships.

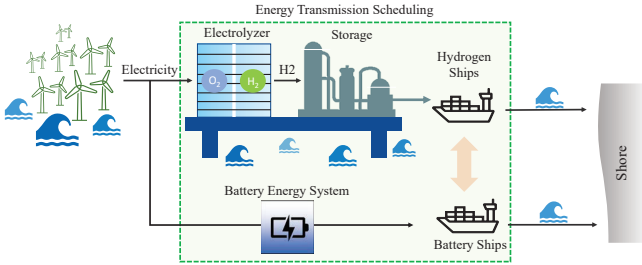


Fig. 1: The concept of integrating an offshore wind farm with hydrogen production and battery storage transportation

The rest of the paper is organized as follows. Section II presents the overall framework of the integration of offshore wind farms using battery/hydrogen ships. Section III shows the results of a case study with different battery and hydrogen ships scheduling strategies. Section IV concludes the paper and discusses potential future works.

II. UNMANNED VESSEL SCHEDULING FOR OFFSHORE WIND INTEGRATION

The hydrogen or battery ships could transfer the generated power from offshore wind farms to the grid or the hydrogen infrastructure. Batteries of a large marine vessel could also be used as back-up supplies, to meet peak demand during disruptive events (e.g., natural disasters) and to manage uncertainties in the network with high penetrations of renewable energy [26]. The main objective function of the vessel scheduling is to maximize the transmission of offshore wind energy. Since the output of the wind farm is varying over time, the charging time

for the battery ships and refilling time for hydrogen tankers would be uncertain. By considering the voyaging constraints of the vessels and discharging time in the shore side, the objective function of the optimization problem could be formulated as follow:

$$\min \sum_{t=1}^T \sum_{s=1}^{N_s} \sum_{h=1}^{N_t} (W(t) - E_h(t) - E_s(t)) \quad (1)$$

where $W(t)$ is the generated power from the offshore wind farm in each hour, s is the index of the number of battery ships, t is the index of the time horizon of the study, and h is the index of the number of hydrogen ships. $E_s(t)$ and $E_h(t)$ represent the stored energy in the battery vessels and consumed power of the electrolyzer for the hydrogen ships at time t , respectively. The mathematical formulation of energy vessel voyaging constraints is provided as follows.

A. General Voyage Constraints

1) *Cruising speed*: Energy vessels usually sail at the cruising speed, which is referred to as the service speed. Cruising speed is generally slower than the high speed, which prepares a smooth and efficient voyage. The speed of the energy vessel can be defined by its operating modes such as cruising, acceleration, and approaching to the harbor. The vessel can move through a secure speed range (2) for safe and efficient sailing [25].

$$\underline{x}_v v_s^{rate} \leq v_s(t) \leq \overline{x}_v v_s^{rate} \quad (2)$$

where \underline{x}_v and \overline{x}_v are the minimum and maximum speed ratio to the rated ship speed v_s^{rate} , respectively.

2) *Cruise voyaging distance*: The cruising distance is modeled in (3), which is formulated based on the ship speed multiplying by the corresponding time. In addition, the necessity for departure from or arrival at certain seaports forces the energy vessel to modify their traveled distance from the rated distance at each time step [27], as modeled in (4).

$$D_s(t) = D_s(t-1) + v_s(t)\Delta t \quad (3)$$

$$\underline{x}_D D_s^{rate} \leq D_s(t) \leq \overline{x}_D D_s^{rate} \quad (4)$$

where \underline{x}_D and \overline{x}_D are the minimum and maximum distance ratio to the rated cruising distance D_s^{rate} , respectively. The total cruising distance depends on the voyaging speed of the energy vessel. In addition, the voyaging distance is formulated as the accumulated distance at each hour, as represented in (3). Furthermore, the departure and arrival of the energy vessel are uncertain. Hence, the distance coverage constraints at the port departure/arrival times are considered in the voyage scheduling, as given in (4).

3) *Vessel propulsion load*: Electric propulsion systems have been becoming popular in the design of future vessels. In this study, an electric propulsion system is considered for the energy vessel movement, where the electric motors are responsible for energy vessel voyaging. The corresponding power consumption is mathematically formulated as a linear function of its speed, as shown in (5).

$$P_{PL}(t) = \alpha_{PL}(v_s(t)) + \beta_{PL} \quad (5)$$

where α_{PL} and β_{PL} are the linear and constant parameters between the propulsion loads and ship cruising speed, respectively. It is worth mentioning that (5) is crucial to the energy management of the energy vessel, since the arrival time of the energy vessel could be modified by adjusting the vessel speed, and different vessel speeds result in various propulsion power demands.

4) *Energy vessel sailing constraints*: Equation (6) ensures that the ship is only in one mode of the operation at each time, either moving (sailing) or connecting to a node (operating) at any time.

$$\sum_{n=1}^N L_{snt} + \sum_{n=1}^{NP} L_{st}^M = 1; \forall s \in S, \forall t \in T \quad (6)$$

where L_{snt} is the status of the s^{th} ship in bus n at time t . If it is located at bus n , L_{snt} is 1; otherwise, it is 0. The parameter of L_{st}^M represents the sailing status of the s^{th} battery/hydrogen ship at time t : 1 if the vessel is connected to node n ; otherwise, 0. Vessels entering and departing constraints are formulated in (7) and (8), respectively. Furthermore, Eq. (9) guarantees that the ship cannot enter and depart at the same time.

$$L_{sn}^D(t) \geq L_{sn}(t-1) - L_{sn}(t); \forall s \in S \quad (7)$$

$$L_{sn}^E(t) \geq L_{sn}(t) - L_{sn}(t-1); \forall s \in S \quad (8)$$

$$L_{sn}^E(t) + L_{sn}^D(t) \leq 1; \forall s \in S \quad (9)$$

where L_{sn}^D and L_{sn}^E are the entrance and departure status of the s^{th} ship at time t , respectively. The value is 1 if the ship is connected to node n , otherwise 0.

B. Hydrogen Electrolyzer System Constraints

The hydrogen electrolyzer and operational constraints of the hydrogen vessels are formulated in this section. The objective of the scheduling of hydrogen ships is to maximize the energy transferring between offshore wind farms and the on-land infrastructure. Hydrogen ships need to consider cruising speed, cruise voyaging distance, propulsion load, and ship sailing constraints as described in Section II-A. In addition to these constraints, several other constraints are also needed for the hydrogen ship.

1) *Capacity constraints*: Because producing hydrogen from wind energy involves the conversion between energy carriers, the electrolyzer units need to be installed in the energy transmission system. In this study, the electrolyzer is installed offshore and the output depends on the power output of the wind farms. In order to avoid any interruption in the production of hydrogen, when the vessels are sailing, a hydrogen storage tank on the offshore side could be considered. The capacity constraints of the hydrogen electrolyzer are listed below:

$$\underline{C}_{el} \leq C_{el} \leq \overline{C}_{el} \quad (10)$$

$$\underline{C}_{tank} \leq C_{tank} + C_{Storage} \leq \overline{C}_{tank} \quad (11)$$

where C_{el} and C_{tank} are the capacity of the electrolyzer and tanks on the hydrogen ships, respectively, and $C_{Storage}$ is the

capability of the offshore hydrogen storage tank. \underline{C} and \overline{C} are the lower and upper limits of the facilities, respectively.

2) *Energy conversion ratio*: Unlike the charging and discharging efficiency of battery ships, hydrogen ships have to convert electricity to hydrogen by the electrolysis of water, and the conversion rate of electricity to hydrogen has to be considered in the model.

$$M_h(t) = E_h(t) \times E^{ratio}(t) \quad (12)$$

where E^{ratio} is the conversion ratio between electricity (kWh) to hydrogen (Kg). E_h and M_h are the hourly electricity used to produce hydrogen and the amount of hydrogen produced, respectively.

3) *Energy balance*: All electrical energy used to produce hydrogen should be less than or equal to the rated power of the wind farm at all time steps.

$$\sum_{e=1}^E P_e \leq P_{wind}; \quad \forall t \in T \quad (13)$$

where P_e and P_{wind} are the electrolyzer and wind farm rated power, respectively.

C. Battery Energy System Constraints

In addition to the general voyage constrained described in Section II-A, additional operational constraints of the battery ships are considered. Each type of battery has a particular set of constraints related to its charging and discharging limits, and charging/discharging control strategy. The battery ship in this study is assumed to have lithium-ion batteries. The charging and discharging limits of the batteries are formulated as follows.

$$PB_s^{DCH} L_{sn}^E(t) \leq PB_s(t) \leq \overline{PB_s}^{DCH} L_{sn}^E(t) \quad (14)$$

where PB is the output power of the battery ship in the discharging status when it is connected to the power grid. The same constraints are applied for the charging status of the battery ship in the offshore wind farm charging side.

The ship energy capacity is the total amount of energy that can be stored in one battery ship. The power capacity is the maximum amount of power that a battery can be charged or discharged. Equation (15) shows the energy capacity of the battery ship at each time step.

$$E_s(t) = E_s(t-1) - PB_s(t) \times ER \quad (15)$$

where ER is total battery energy ratio.

To define the charge and discharge rates of a battery system, the battery capacity (in Ah) is divided by the number of hours taken to charge/discharge the battery. For example, if a battery system has the capacity of 500 Ah and it takes 20 hours to completely discharge the battery, then the discharge rate is defined as 500 Ah / 20 h = 25 A. Thus, based on the input and output current of the battery system, the charging/discharging time of the battery could be calculated. The minimum time

that the battery vessel is connected to the grid (or the offshore wind farm) is presented as follows.

$$BC_s/I_{in}^{wind}(t) = T_s^{disch} \quad (16)$$

$$L_{sn}^E(t) \leq L_s(t + T_{DCH}(s, e)) \quad (17)$$

$$T_{DCH}(s, e) = \begin{cases} e, & e \leq T_s^{disch} \\ 0, & e > T_s^{disch} \end{cases} \quad (18)$$

$$BC_s/I_{out}^{shore}(t) = T_s^{char} \quad (19)$$

$$L_s^D(t) + L_s(t + T_{CH}(s, e)) \leq 1 \quad (20)$$

$$T_{CH}(s, e) = \begin{cases} e, & e \leq T_s^{Char} \\ 0, & e > T_s^{Char} \end{cases} \quad (21)$$

where T_s^{disch} and T_s^{Char} are the minimum discharging and charging time of the battery ship, respectively. BC_s is the capability of the battery vessel, and I_{in}^{wind} is the input current to the vessel from the offshore wind farm, which is dependent on the output of the wind farm. The parameter of I_{out}^{shore} is the output current of the battery vessel on the shore side. When the battery ship is connected to the offshore wind farm to be charged again, the total input energy to the battery ship will be restricted to the hourly output of the wind farm. Equations (16)-(21) model the time charging limits of the battery ship on the offshore wind farm side.

III. CASE STUDY: SIMULATION RESULTS

To evaluate the effectiveness of the proposed unmanned surface vessels for offshore wind integration, a case study is designed to transfer output power of an offshore wind farm to the coastal area. In this case study, the total installed offshore wind power capacity is assumed to be 380 MW. The distance of the wind farm from the shore is assumed to be 50 miles. The minimum and maximum sailing velocities of the vessels are 35 and 55 miles per hour, respectively. The power generation of the offshore wind farm is simulated based on data collected by the U.S. Energy Information Administration (EIA) from the onshore Blue Creek Wind Farm. Modifications have been applied to scale up the onshore wind farm power output to represent offshore wind farm power generation. Figure 2 shows the power output profile of the offshore wind farm during the chosen sample week, represented as the blue curve. To evaluate the effectiveness of different unmanned vessels for transferring offshore wind energy, the following two scenarios are simulated and compared, using: (i) one hydrogen ship in conjunction with offshore hydrogen storage systems, and (ii) one battery ship and one hydrogen ship.

A. Connection of offshore wind farm with a hydrogen ship

An electrolyzer receives power to split water into hydrogen and oxygen. Hydrogen is stored in the tanker of the hydrogen vessels and transferred to shore. To determine the optimal size of the electrolyzer, a mixed-integer linear programming (MILP) problem is formulated in the REopt [28], an open-source techno-economic tool developed by the National Renewable Energy Laboratory, and solved by the FICO Xpress

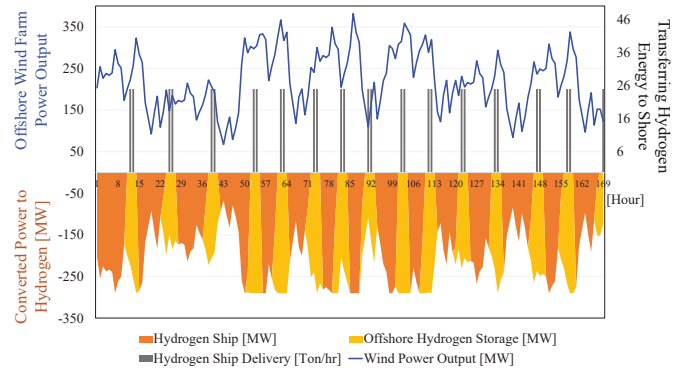


Fig. 2: Hydrogen ship and onsite storage scheduling based on the weekly offshore wind farm power output

solver [29]. The result shows that the optimal installed electrolyzer capacity for the wind farm is 290 MW, in order to maximizing the hydrogen production from the wind power. Two hydrogen storage tanks with a capacity of 50 tons each are considered: one at the offshore wind farm site and one on the hydrogen ship. The electrolyzer rate of producing hydrogen is 20.84 kg/MWh. On average, it takes 12 hours for the hydrogen tank on the site to be filled up. With the two hydrogen storage systems, there is no interruption in producing hydrogen from the wind farm, even during the ship sailing. When the hydrogen ship is on voyaging, the hydrogen would be stored in the offshore tank to be transferred later.

As depicted in the Fig. 2, the orange areas are the power consumption of the electrolyzer to convert electricity to hydrogen. The yellow areas represent the produced hydrogen to be stored in the onsite tank, when the hydrogen vessel is delivering hydrogen at the shore side. By optimizing the schedules of hydrogen vessels and onsite tank, the hydrogen ship could deliver over 97% of the generated energy from the offshore wind farm.

B. Connection of offshore wind farm with hydrogen and battery ships

In this scenario, in addition to the hydrogen ship and onsite hydrogen tanks, a battery ship is added to help transfer the energy. The battery system has a great capability to discharge a large amount of power to the terrestrial network in a short duration of time to help the stability and reliability of the system. The battery ship can also help store sudden peak energy generation from the offshore wind farm and decrease the wind power curtailment. The integration of the battery ship to the power grid could be flexible, depending the grid operational conditions. Especially during disruptive events such as disasters, the battery ship could quickly sail to the affected area to help restoration, thereby enhancing the power grid resilience. On the other hand, the hydrogen ship can store enormous amount of energy compared to battery systems and improve the long-term power network operation. The optimal voyaging of the battery ships is subject to the output of the wind farm and the charge/discharge rates of

TABLE I
Comparing the energy delivery efficiency between the two scenarios

	Generated/transmitted	Efficiency
Wind farm power generation	37,376 MWh	-
Hydrogen ship & onsite tanks	36,307 MWh	97.14%
Hydrogen and battery ships	37,318 MWh	99.81%

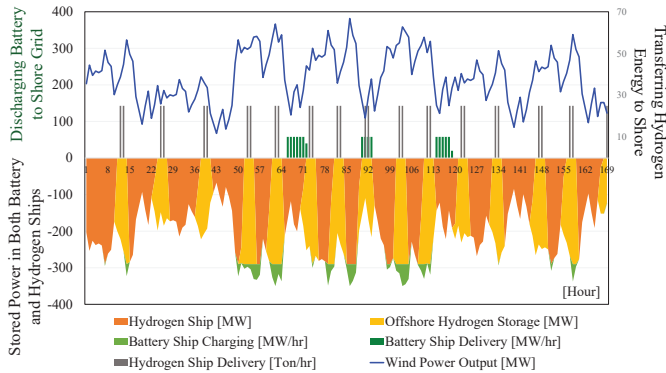


Fig. 3: The scheduling of hydrogen and battery ships based on the weekly offshore wind farm power output

the batteries. In this study, the maximum charging rate of the battery ship is assumed to be 58 MW/hr. The negative zone of the diagrams refers to the charging amount of the energy vessels at the offshore wind farm site, and the positive areas represent delivering and discharging energy to the shore grid. As shown in Fig. 3, during hours where the power output of the wind farm is more than the capability of the electrolyzer, the battery ship could be charged (green areas) to maximize the energy transfer capability. The efficiency of the transmitted energy between the two scenarios is compared in Table I during the entire simulated week. It is observed that by combining the hydrogen ship, battery ship, and onsite hydrogen storage tanks, 99.81% of the offshore wind farm generation could be successfully transmitted to the shore side infrastructure.

IV. CONCLUSION

Offshore wind farms in deep water could generate more energy, which is critical for countries surrounded by deep coastal waters. However, the deep water makes it challenging to use submarine cables (or pipelines) to transfer the wind energy to the shore with electricity (or hydrogen energy) carriers. In this paper, an unmanned surface vessel strategy was proposed to leverage battery and/or hydrogen ships for transmitting offshore wind energy to the seaport infrastructure. Two energy transferring scenarios have been explored in this study by leveraging vessels and onsite hydrogen storage systems. In the first studied scenario, hydrogen electrolyzers are used produce green hydrogen from the offshore wind farm, and one hydrogen ship in conjunction with offshore hydrogen storage systems are utilized for energy transferring. In the second studied scenario, a battery ship is added to help transfer the energy. The integration of the battery ship to the power grid could help enhance the reliability and resilience of the

shoreline power grid during disruptive events. Results show that by combining the hydrogen ship, battery ship, and onsite hydrogen storage tanks, 99.81% of the offshore wind farm generation could be successfully transmitted to the shore side infrastructure.

Battery and hydrogen ships for transmitting offshore wind power could be a promising solution for countries surrounded by deep coastal water, but the technology remains in a relatively early stage of development, which needs to be further evaluated by considering more factors. For example, potential future work will (i) evaluate the economic benefits of using unmanned vessels, and (ii) take into account the uncertainties in the voyaging and study their impacts on the scheduling of energy vessels.

ACKNOWLEDGMENT

This material is based upon work sponsored by the Department of the Navy, Office of Naval Research under ONR award number N00014-20-1-2795. The United States Government has a royalty-free license throughout the world in all copyrightable material contained herein. Any opinions, findings, and conclusions or recommendations expressed in this material are those of the author(s) and do not necessarily reflect the views of the Office of Naval Research.

REFERENCES

- [1] M. Froese, "Global offshore wind capacity grew nearly 10% in first half of 2019," 2019. [Online]. Available: <https://www.windpowerengineering.com/global-offshore-wind-capacity-grew-nearly-10-in-first-half-of-2019/>
- [2] D. Radu, M. Berger, A. Dubois, R. Fonteneau, H. Pandžić, Y. Dvorkin, Q. Louveaux, and D. Ernst, "Assessing the impact of offshore wind siting strategies on the design of the european power system," *Applied Energy*, vol. 305, p. 117700, 2022.
- [3] W. House, "Fact sheet: Biden administration jumpstarts offshore wind energy projects to create jobs," 2021.
- [4] J.-S. Shin and J.-O. Kim, "Optimal design for offshore wind farm considering inner grid layout and offshore substation location," *IEEE Transactions on Power Systems*, vol. 32, no. 3, pp. 2041–2048, 2017.
- [5] A. Dunham, J. Pegg, W. Carolsfeld, S. Davies, I. Murfitt, and J. Boutilier, "Effects of submarine power transmission cables on a glass sponge reef and associated megafaunal community," *Marine Environmental Research*, vol. 107, pp. 50–60, 2015.
- [6] D. Fey, M. Greszkiewicz, Z. Otremba, and E. Andrulewicz, "Effect of static magnetic field on the hatching success, growth, mortality, and yolk-sac absorption of larval northern pike esox lucius," *Science of The Total Environment*, vol. 647, pp. 1239–1244, 2019.
- [7] S. McDonagh, S. Ahmed, C. Desmond, and J. D. Murphy, "Hydrogen from offshore wind: Investor perspective on the profitability of a hybrid system including for curtailment," *Applied Energy*, vol. 265, p. 114732, 2020.
- [8] G. Calado and R. Castro, "Hydrogen production from offshore wind parks: Current situation and future perspectives," *Applied Sciences*, vol. 11, no. 12, 2021.
- [9] A. Taieb and M. Shaaban, "Cost analysis of electricity transmission from offshore wind farm by hvdc and hydrogen pipeline systems," in *2019 IEEE PES GTD Grand International Conference and Exposition Asia (GTD Asia)*, 2019, pp. 632–636.
- [10] M. Sclaro and N. Kittner, "Optimizing hybrid offshore wind farms for cost-competitive hydrogen production in germany," *International Journal of Hydrogen Energy*, vol. 47, no. 10, pp. 6478–6493, 2022.
- [11] O. S. Ibrahim, A. Singlitico, R. Proskovics, S. McDonagh, C. Desmond, and J. D. Murphy, "Dedicated large-scale floating offshore wind to hydrogen: Assessing design variables in proposed topologies," *Renewable and Sustainable Energy Reviews*, vol. 160, p. 112310, 2022.

- [12] T. R. Lucas, A. F. Ferreira, R. Santos Pereira, and M. Alves, "Hydrogen production from the windfloat atlantic offshore wind farm: A techno-economic analysis," *Applied Energy*, vol. 310, p. 118481, 2022.
- [13] Y. Jiang, W. Huang, and G. Yang, "Electrolysis plant size optimization and benefit analysis of a far offshore wind-hydrogen system based on information gap decision theory and chance constraints programming," *International Journal of Hydrogen Energy*, vol. 47, no. 9, pp. 5720–5732, 2022.
- [14] P. Leahy, E. McKeogh, J. Murphy, V. Cummins *et al.*, "Development of a viability assessment model for hydrogen production from dedicated offshore wind farms," *International Journal of Hydrogen Energy*, vol. 46, no. 48, pp. 24620–24631, 2021.
- [15] C. N. Bonacina, N. B. Gaskare, and G. Valenti, "Assessment of offshore liquid hydrogen production from wind power for ship refueling," *International Journal of Hydrogen Energy*, vol. 47, no. 2, pp. 1279–1291, 2022.
- [16] Y. Wu, F. Liu, J. Wu, J. He, M. Xu, and J. Zhou, "Barrier identification and analysis framework to the development of offshore wind-to-hydrogen projects," *Energy*, vol. 239, p. 122077, 2022.
- [17] Y. Jiang, W. Huang, and G. Yang, "Electrolysis plant size optimization and benefit analysis of a far offshore wind-hydrogen system based on information gap decision theory and chance constraints programming," *International Journal of Hydrogen Energy*, vol. 47, no. 9, pp. 5720–5732, 2022.
- [18] S. Song, H. Lin, P. Sherman, X. Yang, C. P. Nielsen, X. Chen, and M. B. McElroy, "Production of hydrogen from offshore wind in china and cost-competitive supply to japan," *Nature communications*, vol. 12, no. 1, pp. 1–8, 2021.
- [19] Y. Yan, H. Zhang, Q. Liao, Y. Liang, and J. Yan, "Roadmap to hybrid offshore system with hydrogen and power co-generation," *Energy Conversion and Management*, vol. 247, p. 114690, 2021.
- [20] R. d'Amore Domenech, T. J. Leo, and B. G. Pollet, "Bulk power transmission at sea: Life cycle cost comparison of electricity and hydrogen as energy vectors," *Applied Energy*, vol. 288, p. 116625, 2021.
- [21] K. Hein, Y. Xu, W. Gary, and A. K. Gupta, "Robustly coordinated operational scheduling of a grid-connected seaport microgrid under uncertainties," *IET Generation, Transmission & Distribution*, vol. 15, no. 2, pp. 347–358.
- [22] S. Badakhshan, S. Senemmar, and J. Zhang, "Dynamic feasibility assessment of ship-to-grid interconnection by dc-link," in *2022 IEEE Texas Power and Energy Conference (TPEC)*, 2022, pp. 1–6.
- [23] G. Guidi, J. A. Suul, F. Jensen, and I. Sornfon, "Wireless charging for ships: High-power inductive charging for battery electric and plug-in hybrid vessels," *IEEE Electrification Magazine*, vol. 5, no. 3, pp. 22–32, 2017.
- [24] S. Karimi, M. Zadeh, and J. A. Suul, "A multi-layer framework for reliability assessment of shore-to-ship fast charging system design," *IEEE Transactions on Transportation Electrification*, pp. 1–1, 2021.
- [25] R. Smolenski, G. Benysek, M. Malinowski, M. Sedlak, S. Stynski, and M. Jasinski, "Ship-to-shore versus shore-to-ship synchronization strategy," *IEEE Transactions on Energy Conversion*, vol. 33, no. 4, pp. 1787–1796, 2018.
- [26] M. Dabbaghjamesh, S. Senemmar, and J. Zhang, "Resilient distribution networks considering mobile marine microgrids: A synergistic network approach," *IEEE Transactions on Industrial Informatics*, vol. 17, no. 8, pp. 5742–5750, 2021.
- [27] Z. Li, Y. Xu, S. Fang, Y. Wang, and X. Zheng, "Multiobjective coordinated energy dispatch and voyage scheduling for a multienergy ship microgrid," *IEEE Transactions on Industry Applications*, vol. 56, no. 2, pp. 989–999, 2020.
- [28] K. Anderson, D. Olis, B. Becker, L. Parkhill, N. Laws, X. Li, S. Mishra, T. Kwasnik, A. Jeffery, E. Elgqvist *et al.*, "Reopt lite user manual," National Renewable Energy Lab.(NREL), Golden, CO (United States), Tech. Rep., 2021.
- [29] H. Li, J. Rahman, and J. Zhang, "Optimal planning of co-located wind farm and hydrogen plant: A techno-economic analysis," in *Journal of Physics: Conference Series*. Delft, Netherlands: The Science of Making Torque from Wind (TORQUE 2022), 2022.